Advances in Pavement Design through Full-scale Accelerated Pavement Testing – Jones, Harvey, Mateos & Al-Qadi (Eds.)
© 2012 Taylor & Francis Group, London, ISBN 978-0-415-62138-0

Use of mechanistic-empirical performance simulations to adjust and compare results from accelerated pavement testing

J.T. Harvey, D. Jones, J.D. Lea & R.Z. Wu
University of California Pavement Research Center, University of California, Davis

P. Ullidtz
Consultant, Copenhagen, Denmark

B. Tsai
University of California Pavement Research Center, University of California, Berkeley

ABSTRACT: This paper presents a discussion of the use of Mechanistic-Empirical (ME) analysis to simulate Accelerated Pavement Testing (APT) results in order to overcome problems with using APT data, such as differences in underlying conditions, construction quality, loading, and environmental control. This is particularly important when APT results are used for comparison studies between different pavement alternatives. In the process presented, APT results are first used to calibrate ME models so that the results from simulation of APT under actual conditions match the results predicted by the models. The APT results are then simulated with ME, this time assuming uniform conditions in the APT, to produce a ranking of the alternatives tested without the bias of differences between APT sections. Extrapolation of APT results to field conditions using ME analysis is also discussed. The paper presents a demonstration of this process from an experiment to compare different asphalt overlay treatments for reflective cracking and rutting performance.

1 INTRODUCTION

1.1 *Why are mechanistic-empirical simulations of APT results needed?*

Accelerated Pavement Testing (APT) is performed for a number of reasons. One of the most common is to quickly evaluate a new pavement technology that has shown promise in the laboratory and mechanistic analysis before going to more widespread implementation or pilot projects on the road network. The evaluation usually involves comparison with proven existing pavement technologies. Often there is some performance data from initial pilot projects in the field. However, the results from the field pilot projects are sometimes inconclusive for one or more of the following reasons:

- Differences in construction quality between the different sections, or problems with construction,
- Differences in the underlying pavement structure make direct comparison difficult,
- Insufficient time for the pavements to reach failure,
- Different traffic or climate from the control sections that new technologies are being compared to, because the pilot sections are in a different location,
- Pilot projects were placed in a location that is low risk in case of early failure (usually in a low traffic location), while the primary application will be in a different climate region or traffic level.

APT experiments intended to compare different types of pavement are often affected by the first and second problems listed above, which makes it difficult to provide a completely unbiased comparison. These problems occur because it is nearly impossible to construct exactly replicate subgrade and underlying pavement structures, achieve the same concrete curing conditions because of moisture and temperature differences at different times, or obtain the same compaction of asphalt, on different sections. These often occur because of factors such as the inevitable breakdowns at the materials plant, paver problems, clogged jets on the tack coat spray truck, and lost trucks full of hot asphalt or hydrating concrete.

In the process described in this paper, mechanistic-empirical (ME) models are used to help produce a ranking of the alternatives tested in an APT comparison study by accounting for the bias caused by differences in conditions that occurred between APT sections through ME simulation.

1.2 *Interaction between mechanistic-empirical analysis and APT*

The most common interaction of ME and APT has been the use of APT to calibrate ME models. Many mechanistic-empirical (ME) pavement design methods have been calibrated using at least some APT

data over the years. These include a number of the early methods that were calibrated in part using the AASHTO Road Test data, as well as more recent methods such as the AASHTO *Darwin*-ME models and software (*Mechanistic-Empirical Pavement Design Guide* [*MEPDG*], based on the NCHRP 1-37A [ARA, 2004]) and the *CalME* models and software (Ullidtz, 2008a, 2008b, 2010) that are the subject of this paper.

A less common interaction of ME and APT is to use ME to adjust APT results to help remove bias in APT comparison studies caused by the differences in construction, underlying structure, trafficking, and environmental control. The process for doing this was described in Harvey (2008) as follows:

"Once [ME] models are reasonably well validated and calibrated, they can be used to "re-run" the APT test sections through simulation with completely equal underlying conditions, temperature, water content, etc. Because there are inevitable differences in conditions that are supposed to be equal between APT sections, this simulation of the APT tests is extremely useful to confirm that the results of the initial empirical comparisons of performance do not change significantly under absolutely uniform conditions."

The synergetic interaction between APT and ME is greatly improved when the ME analysis method, such as the one used in this study, is capable of simulating the entire process of pavement damage and aging (or curing), and the changes in corresponding stress and strain responses throughout the entire pavement life for both the APT section and simulated field sections. This is very difficult to accomplish if the ME analysis method uses an approach, such as Miner's Law, that only considers the initial condition of the pavement and the final failure state. With the latter type of approach the ME method can only be calibrated based on the stress and strain responses at the initial state and the final failure distress level. The responses that occur in between these two points in time cannot be verified with data from APT instrumentation.

For example, the *MEPDG* (ARA, 2004) produces calculations of fatigue damage for the entire simulation starting from the first load. However, the asphalt master curve is not updated for damage (loss of stiffness for a given load, time of loading, and temperature) after each set of loads in each time increment (month) and responses of the pavement (stresses and strains) calculated for the undamaged state are therefore used for the simulation of the entire life of the pavement. (Note that although the master curve is not updated for damage, it is updated for aging so that the *MEPDG* predicts an increase in asphalt stiffness until the end of life, at which time the total damage calculated by Miner's Law is applied). Alternatively, a fully "incremental-recursive" analysis method (described in more detail in Ullidtz [2008a, 2008b]) is defined as one where the material properties are updated for damage, aging, and other processes (such as debonding) incrementally throughout the section life. With an incremental-recursive method, responses measured with APT instrumentation at intervals during the entire APT test can be used to calibrate and verify the damage processes simulated by the ME analysis method because they both reflect the incremental damage occurring during loading. The *CalME* analysis models used in the study described in this paper use an incremental-recursive method that updates the condition (fatigue and permanent deformation) of each layer of the pavement after each increment of loading for both aging and damage using the time hardening approach. Examples of the load increment can be each hour of a representative day of every month of the life for simulations of field loading, or each hour in an APT test. An additional advantage of incremental-recursive models is that data from APT and long-term pavement performance (LTPP) sections that never demonstrate distress on the surface can be used for calibration of the models because the damage (measured in terms of loss of stiffness such as in the asphalt master curve) can be measured by backcalculating the stiffness from measured deflections or strains and comparing it with the initial undamaged stiffness under the same load, time of loading, and temperature conditions. For example, some of the Heavy Vehicle Simulator (HVS) test sections in the study described in this paper never exhibited surface cracking, but had measurable damage to pavement layers backcalculated from deflections.

This paper presents an example of the three main steps in using an ME analysis method in conjunction with APT to greatly increase the benefit obtained from both of these research and development tools. These steps are:

1. Calibrate and verify the damage process models in the ME analysis method using instrumented APT data from the as-built comparison test sections and actual testing conditions (loading, temperature and moisture primarily). Once this is completed, the ME analysis should be capable of simulating the performance of the pavement test sections under a range of conditions.
2. Simulate the APT comparison test sections again, assuming exactly the same as-built structures, as-built construction quality, and as-tested loading, temperature, and moisture conditions. This will provide a "fair" comparison between alternatives tested under simulated equal conditions.
3. Simulate field sections for the same comparison of different pavements under different conditions of climate, traffic, materials, thicknesses, construction quality, and subgrade. This is essentially an extrapolation of the APT results, which must be treated with some caution and pavement engineering judgment. However, these simulations can be extremely useful because extreme temperature, loading, and moisture conditions are often used to accelerate pavement damage in APT and more realistic estimates are desired for the range of typical condition on the network.

2 OVERVIEW OF THE PROJECT AND APT RESULTS

The objective of the project used as an example in this paper was to develop improved rehabilitation treatments for reflective cracking for California, while also determining the risk of rutting for those treatments (Jones, et al., 2007a, 2008). Simulation of fatigue cracking of the original pavement prior to rehabilitation was also performed to help calibrate the ME models used for the evaluation of the rehabilitation treatments (Jones, et al., 2007b).

To provide a platform for evaluation of the rehabilitation treatments, a pavement was built to a single design on a compacted clay subgrade. The pavement was large enough (two lanes each 3.7 m wide by 80 m long) to provide adequate area for later placement of representative samples of six rehabilitation overlays with five different types of material produced at a commercial asphalt plant. All of the construction was performed using full-scale highway construction equipment, procedures and specifications using a qualified contractor selected based on low-bid.

The initial pavement was designed following standard Caltrans procedures and incorporated a 410 mm Class 2 aggregate base with a 90 mm dense-graded asphalt concrete (DGAC) surface. As was allowed by Caltrans District specifications, the Class 2 aggregate base included building waste, primarily crushed concrete, which was shown in the forensic trenching to still have reactive properties (Jones and Harvey, 2007c). The base was later found to have increased stiffness when left to cure with the light cementation coming from unhydrated cement in the crushed concrete that was activated by compaction water. The increased stiffness was substantially broken down when subjected to HVS loading, and showed renewed increases in stiffness whenever HVS loading was stopped, such as between completion of the initial cracking of the underlying pavement and the subsequent loading of the same locations after the overlay to test for reflective cracking. Six replicate sections of this structure were trafficked with the HVS between 2001 and 2003 to induce fatigue cracking in the DGAC. This trafficking of the initial pavement is summarized in Table 1, along with the overlay type later placed on the cracked DGAC pavement in each section.

Table 1. Summary of testing on the underlying DGAC layer and identification of overlay sections.

Under section	Load reps[1]	Final rut depth mm	Final crack density m/m^2	Overlay	overlay section
567RF	78,500	13.7	8.1	MB15-G	586RF
568RF	377,556	14.2	5.5	RAC-G	587RF
569RF	217,116	3.8	5.9	AR4000-D	588RF
571RF	1,101,553	14.1	6.2	MB4-G2	589RF
572RF	537,074	8.8	8.1	MB4-G3	590RF
573RF	983,982	15.3	4.1	MAC15-G	591RF

[1]at 20°C, 60 kN dual wheel load, 720 kPa tire pressure, bi-directional loading; [2]45 mm [3] 90 mm

The cracked DGAC sections were overlaid with six different treatments, with all but one placed with a thickness of half of the underlying DGAC (one type of asphalt overlay material was also constructed with full thickness) to assess their ability to limit reflective cracking. The treatments included:

- Half-thickness (45 mm) MB4-G gap-graded overlay, with a terminal blend rubberized binder containing both polymer and an unspecified amount of recycled tire rubber, and meeting Caltrans MB-4 binder specification;
- Full-thickness (90 mm) MB4-G gap-graded overlay;
- Half-thickness MB4-G gap-graded overlay with a terminal blend rubberized binder with minimum 15 percent recycled tire rubber (referred to as "MB15-G" in this paper);
- Half-thickness MAC15TR gap-graded overlay with a terminal blend rubberized binder with minimum 15 percent recycled tire rubber, similar to the MAC-10TR binder specified in the Southern California Greenbook section 600-5.2.1, except that it uses 15 percent tire rubber rather than 10 percent tire rubber. (referred to as "MAC15-G" in this paper);
- Half-thickness rubberized asphalt concrete gap-graded overlay (RAC-G) using a "wet" process binder containing at least 18 percent recycled tire rubber, included as a control for performance comparison purposes, and
- Full-thickness (90 mm) dense DGAC overlay with a conventional AR-4000 binder (now PG64-16), included as a control for performance comparison purposes.

Each of the overlay treatments was subjected to two APT tests. The first test was performed at high temperatures (asphalt heated to 50°C at 50 mm depth) to assess rutting performance. The second test was performed at moderate temperatures (asphalt temperature maintained at 20 C at 50 mm depth) on the overlay directly above the previously cracked underlying pavement section to assess reflective cracking. Table 2 shows the details of the APT tests on the overlays. A summary of the experiment and references to other project reports can be found in Jones et al. (2007a).

The results of the APT tests for rutting of the overlay are summarized in Table 3. It can be seen that the control overlays in the experiment typically used by Caltrans, conventional dense-graded overlay and RAC-G, were in the top three for best rutting performance, while the terminal blend mixes ranked second, fourth, fifth and sixth. These results suggested that caution should be used for placement of these mixes in locations with a higher risk of rutting based on the then current mix designs.

Table 2. Summary of HVS loading program on overlays.

Test Type	Section	Start Repetition	Total Repetitions	Wheel Load (kN)	ESALs	Temperature °C
Rutting	580RF	Full test	2,000	60	11,000	50°C ± 4°C
	581RF		7,600		42,000	
	582RF		18,564		102,000	
	583RF		15,000		83,000	
	584RF		34,800		191,000	
	585RF		3,000		17,000	
Reflective cracking	586RF (MB15-G)	0	2,492,387	60	88 million	20°C ± 4°C to one million repetitions;
		215,000		90		
		410,000		80		
		1,000,001		100		
	587RF (RAC-G)	0	2,024,793	60	66 million	
		215,000		90		
		410,000		80		
		1,000,001		100		
	588RF (AR4000-D)	0	1,410,000	60	37 million	
		215,000		90		
		410,000		80		
		1,000,001		100		
	589RF (45 mm MB4-G)	0	2,086,004	60	69 million	15°C ± 4°C the reafter
		215,000		90		
		407,197		80		
		1,002,000		100		
	590RF* (90 mm MB4-G)	0	1,981,365	60	37 million	
		1,071,004		90		
		1,439,898		80		
		1,629,058		100		
	591RF (MAC15-G)	0	2,554,335	40	91 million	
		215,000		60		
		410,000		80		
		1,000,001		100		

*590RF was the first HVS test on the overlays, and the 60 kN loading pattern was retained for an extended period to prevent excessive initial deformation (rutting) of the newly constructed overlay.

Table 3. Overlay rutting study results.

Overlay	rank	Reps to 12.5 mm avg max rut	Avg. max rut (mm)[1]	Avg. down rut (mm)
AR4000-D	1	8,266	15.6	8.1
MB4-G (45)	2	3,043	31.3	9.7
RAC-G	3	2,324	22.7	10.3
MB4-G (90)	4	1,522	23.3	11.9
MB15-G	5	914	18.8	7.1
MAC15-G	6	726	23.5	7.7

[1]Rut measured from highest point of upheaval to lowest point of deformation.

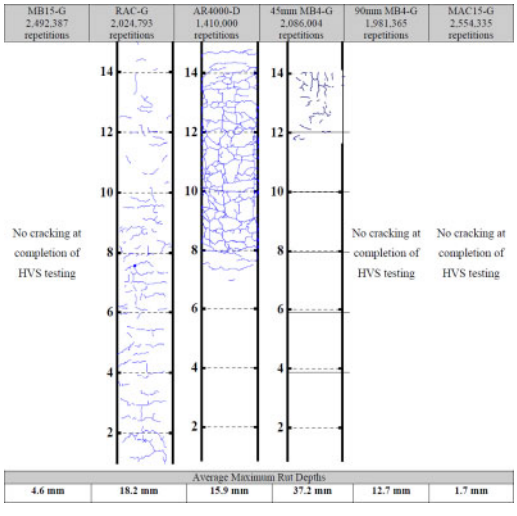

Figure 1. Cracking patterns and rut depths on the overlay sections.

With regard to reflective cracking, after millions of load repetitions, only three of the overlay sections showed surface cracking (DGAC, RAC-G and a small area of the MB15-G), as shown in Figure 1. The sub-sections with different levels of cracking seen in Figure 1 were modeled as separate sections. The other three sections had measureable damage, identified by increased deflections. The terminal blend overlay sections had the best reflective cracking performance with only one showing any surface cracking after more than two million load repetitions. Forensic trenches after HVS testing showed that all of the surface cracks were reflected from the cracked underlying DGAC, and that some of the DGAC cracks had begun to propagate

upward but had not reached the surface in the overlay sections that did not show surface cracking.

3 SIMULATIONS

Six sets of simulations were performed using the California mechanistic-empirical design and analysis software *CalME*, including five of the HVS tests and a sixth on a hypothetical set of typical Caltrans structures and traffic conditions in different climate regions in the state. The simulations are summarized as follows (Jones et al., 2007b):

1. Simulation of the tests on the original pavement structure using actual (in-situ) conditions;
2. Simulation of the moderate-temperature cracking tests on the overlaid pavement structure using actual conditions;
3. Simulation of the high-temperature rutting tests on the overlaid pavement structure using actual conditions;
4. Simulation of the high-temperature rutting tests on the overlaid pavement structure using design thicknesses for the overlays and identical conditions of underlying pavement structure and temperature across all of the tests;
5. Simulation of the moderate-temperature cracking tests on the overlaid pavement structure using design thicknesses for the overlays and identical conditions of underlying pavement structure and temperature across all of the tests; and
6. Simulation of rutting and cracking for a hypothetical set of typical Caltrans structures and traffic conditions in different climate regions in the state.

The first three sets of simulations served to validate the *CalME* models by comparing the calculated results from *CalME* models with the measured responses and performance. Simulations 4 and 5 provided objective ranking of the different asphalt overlays without the influence of underlying conditions, which varied in the actual HVS tests. The sixth set of simulations provided extrapolation of the HVS results to field conditions and an understanding of the sensitivity of the predicted performance of the different overlays.

3.1 *Input data and methodology*

To perform the simulations using actual conditions, data from each HVS test, reported in a series of first-level analysis reports (Jones, et al., 2007a), were imported into a *CalME* database. The data comprised information on loads (time of application and load level), temperatures at different levels, road surface deflectometer (RSD) results, multi-depth deflectometer (MDD) resilient and permanent deformations, and pavement profiles. Strain gauges were not used for the overlay testing because the cracking of the overlays was due to localized strains above cracks causing reflective cracking, not overall bending of the overlays. In fact, the bottoms of many of the thin overlays would have been above the neutral axis and in compression if analyzed using layer-elastic theory, but with high tensile and shear strains above the cracks.

The backcalculated layer moduli from the last falling weight deflectometer (FWD) tests undertaken before commencement of HVS loading on each section were used as the initial asphalt concrete layer moduli (reference temperature of 20°C). The master curve for the asphalt concrete layers was obtained from frequency sweep tests on beams in the laboratory, with the exception of the original DGAC layer where the master curve was based on FWD backcalculated moduli. The change in stiffness of the subgrade with changing stiffness of the pavement layers and with changing load level was obtained from FWD backcalculated values. These parameters were used with the layer-elastic response model to calculate stresses, strains, and deflections in the pavement structure. The tensile strain in an overlay over an existing cracked asphalt concrete layer was calculated using a regression equation based on finite element method modeling described in Ullidtz (2008a, 2010).

A number of models were used to predict the pavement performance, in terms of cracking and permanent deformation. Parameters for prediction of asphalt concrete damage for bottom up cracking (from the underlying DGAC sections) and reflective cracking (overlays) were obtained from controlled strain four-point fatigue tests on beams (AASHTO T 321). The model for the damaged asphalt master curve has the format:

$$\log(E)=\delta+\frac{\alpha\times(1-\omega)}{1+\exp(\beta+\gamma\log(tr))} \quad (1)$$

which is the *MEPDG* asphalt master curve equation for dynamic stiffness (E) where a, b, g and d are fitting parameters, tr is the reduced time of loading, and the damage (ω), is a function of the number of loads, the tensile strain, and current modulus.

Cracking at the pavement surface was calculated from the damage to the surface layer, using models shown below relating damage (ω) to crack initiation and crack propagation developed based on previous simulations of HVS tests and the FHWA WesTrack experiment in Nevada (Ullidtz, 2008b)) to initially simulate cracking from HVS testing on the underlying pavement and the later overlays. These parameters did not predict the relationship of damage to surface cracking for the overlays and were then re-calibrated to match the reflective cracking results on the overlays tested, resulting in the following:

$$\omega_{initiation}=\frac{0.42}{1+\left(\frac{h_{AC}}{250mm}\right)^{0}} \quad (2)$$

$$Crm/m^2=\frac{10}{1+\left(\frac{\omega}{\omega_o}\right)^{-3.8}} \quad (3)$$

Where $\omega_{initiation}$ is the damage at crack initiation, hAC is the thickness of the combined asphalt layers, Crm/m^2 is the crack density, and other values are calibrated constants.

Repeated simple shear tests at constant height (RSST-CH, AASHTO T 320) were used to determine the parameters for predicting permanent deformation in the asphalt concrete layers.

A crushing model was developed for the lightly cemented base layer, consisting of recycled material with a high content of old crushed concrete. The model was based on a model developed for cement-treated bases (CTB) at an HVS-Nordic experiment (Thoegersen et al., 2004). A model developed for subgrade materials in the Danish Road Testing Machine was used for permanent deformation of the unbound layers.

An incremental-recursive process in *CalME* was used to simulate the performance of the test sections. A one-hour time increment was used for the HVS test simulations. The modulus of the subgrade was adjusted to the stiffness of the pavement layers and to the load level. Wander was considered for the cracking sections, while the rutting sections had channelized traffic. For all load positions, the stresses and strains at the center line of the test section were calculated and used to determine the decrease in moduli and the increase in permanent deformation of each of the pavement layers. The output from these calculations were used, recursively, as input to the calculation for the next hour of loading, using a time hardening procedure, which takes changes in moduli, response, damage, and permanent deformation into consideration.

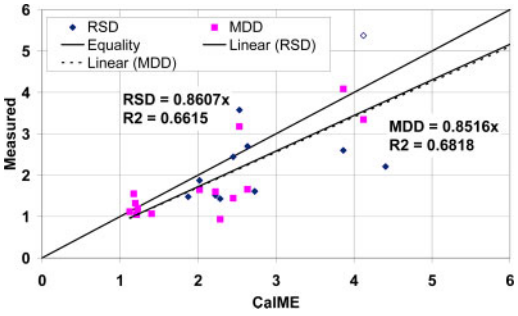

Figure 2. Increase in deflection (terminal deflection/initial deflection) during HVS experiments, as simulated and measured. (Note: some sections had both RSD and MDD measurements, others only one or the other, see Jones, et al., (2007b) for detailed results).

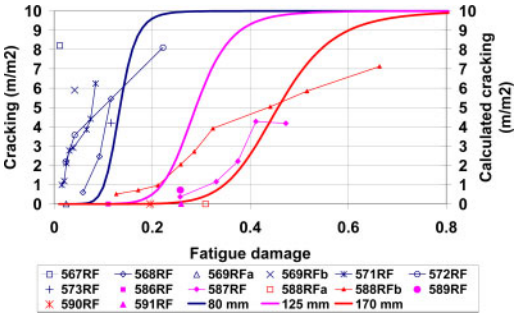

Figure 3. Observed surface cracking vs. damage for HVS tests on underlying DGAC and overlays with original parameters.

3.2 *Responses*

The first step in the simulation ensures that the calculated pavement response was reasonably close to the actual pavement response during the test. The calculated pavement response was used to predict the pavement performance (damage and permanent deformation) and if this response was not reasonably correct it would be futile to use it for calibration of the performance models. In this study, response measurements included resilient MDD deflections and/or RSD deflections.

Once the resilient deflections were predicted with reasonable accuracy during the simulations, the performance models were calibrated such that the permanent deformation of each layer, the decrease in layer moduli, and the observed surface cracking, were reasonably well predicted. The first important step in the simulations was to obtain good backcalculated stiffness values for all layers, and to compare those with measured values and laboratory test data. The best impression of the agreement (or lack of agreement) between the measured and calculated values is obtained from the deflection measurements from the entire duration of the HVS tests from start to finish, taken at various times during each test, which are shown in Jones et al., (2007b). A summary of the change in surface deflections between the initial and final deflections from HVS tests on both the underlying cracking tests and the cracking tests on the overlays from both MDD (one location) and RSD (average of 13 locations) measurements is provided in Figure 2. *CalME* tends to slightly overestimate the increase in deflection. The uncertainty on the measured values is illustrated by the difference between the deflections measured by the RSD and by the MDD, which in some cases is quite large.

3.3 *Simulations 1 and 2: Fatigue damage and cracking of asphalt concrete layers under actual conditions*

The damage calculated by *CalME* compared to the observed cracking on the test sections was reasonably accurate (see Figure 3), but the results were influenced by differences in the modulus of the underlying DGAC determined from FWD backcalculation and those determined from laboratory frequency sweep testing. This difference was attributed to early damage of the DGAC layer. Figure 4 shows that the surface cracking was fairly well predicted for the underlying sections (Sections 567 through 573) by cracking

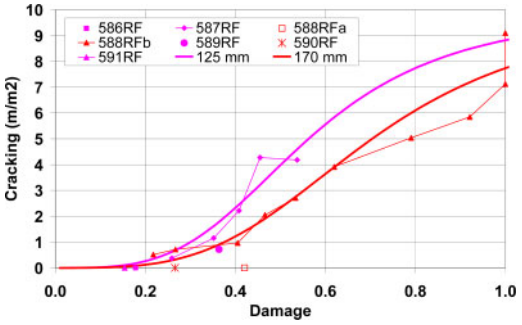

Figure 4. Observed surface cracking versus damage for overlays calculated using re-calibrated damage to cracking equation parameters to better fit overlay results.

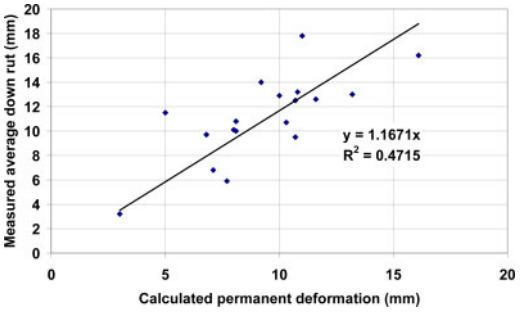

Figure 5. Calculated overall permanent deformation versus measured final down rut.

equation parameters that had been developed previously from other APT results, but not as well for the overlay reflective cracking sections that had surface cracking (Sections 587 through 589). In the figure the *CalME* calculation for a thickness of 80 mm should be compared with the HVS results for the underlying sections; the *CalME* calculation for a thickness of 125 mm should be compared to the 45 mm overlay results, and the *CalME* calculation for a thickness of 170 mm should be compared to the 90 mm overlay results, since those are the approximate thicknesses of the combined asphalt layers in each case.

In order to obtain a better fit to the measured reflective cracking in the overlay sections, the parameters in the equations developed for crack initiation and crack propagation that relate damage to surface cracking in *CalME* were re-calibrated in a series of iterations, using different constants. Cracking predicted using the re-calibrated equations is compared to the measured cracking for the overlays in Figure 4.

3.4 *Simulation 3: Permanent deformation under actual conditions*

The terminal overall permanent deformation calculated by *CalME* at the end of each HVS test and the average measured down rut (same as average deformation in Table 1) from profile measurements are shown in Figure 5. A similar plot for final down rut versus the permanent deformation of the top cap of the MDDs had a poorer correlation with *CalME* results because most of the permanent deformation was in the asphalt layer which was not captured because of positioning of the MDD sensors.

On average, *CalME* underestimated the overall permanent deformation by about seven percent, but the correlation coefficient was quite low. This should be seen in the light of the very large variation of down rut within some of the HVS sections. A difference of 5 mm to 10 mm between the minimum and the maximum down rut measured within the 6.0 m long test section was not unusual, and in one case (45 mm MB4-G) it reached 30 mm.

The permanent deformation of the top MDD includes the permanent compression of the aggregate base layers and the permanent deformation of the subgrade. The permanent deformation of the subgrade was usually very low, less than 1.0 mm, except for one section where one of the MDDs recorded final permanent deformations at the subgrade of 2.5 mm and another that recorded a value of 1.5 mm. In both cases, however, another MDD in the section recorded a permanent deformation close to zero.

3.5 *Simulation 4: Permanent deformation in overlaid sections with uniform conditions*

Experience has shown that the HVS testing conditions always have some influence on the performance of a particular section. This influence increases with increasing duration of the test. The rutting study was considered to consist of short duration tests since the test sections were on parts of the overlays that had not been trafficked previously with the HVS. As a consequence, the influence of the test conditions was less pronounced than it was in the fatigue experiment, which had a longer duration and took place on test sections located precisely above those trafficked with the HVS during Phase 1 of the experiment (HVS test on underlying DGAC). For completeness, the simulations were repeated for the rutting experiment using the same underlying structure used for the reflective cracking study discussed above, with the exception that the modulus of the underlying asphalt was assumed to be 3,200 MPa at 20°C, corresponding to the approximate layer moduli determined from FWD tests. The pavement structure and test conditions for HVS Test 584RF (90-mm MB4-G) were used for the simulation of uniform conditions. Almost 20,000 load repetitions (60 kN) were applied to this section. The ranking from best to worst was:

1. 90 mm MB4-G
2. AR4000-D (DGAC control)
3. RAC-G (control)
4. MAC15-G
5. 45 mm MB4-G
6. MB15-G

Table 4. Ranking of overlays for reflective cracking under uniform conditions.

Layer	Damage	Cracking (m/m^2)	Rank	
MAC15-G (591)	(45 mm)	0.48	3.1	1
MB4-G (589)	(45 mm)	0.56	5.0	2
MB4-G (590)	(90 mm)	0.75	5.5	3
MB15-G (586)	(45 mm)	0.69	6.7	4
RAC-G (587)	(45 mm)	0.76	7.4	5
AR4000 (588)	(90 mm)	1.00	7.7	6

This ranking differs from the actual results as can be seen by comparison with actual results in Table 3. Some mixes changed ranking by one place, and one mix changed ranking by two places.

3.6 *Simulation 5: Fatigue damage and cracking from reflection of overlays under uniform conditions*

Although the original pavement was built to provide uniform support for the reflective cracking study, the forensic investigation showed that there was some variation over the length of the structure, specifically with regard to layer thickness, composition of the recycled aggregate, and degree of re-cementation of the aggregate particles. The conditions of the underlying structure, wheel loads, and climate should be identical when ranking the different overlays. The simulations were therefore repeated using uniform conditions. The HVS loading and climate for Section 591RF (MAC15-G) were used, but the number of load applications was multiplied by 50. Thicknesses of 45 mm, 80 mm, and 400 mm were used for the overlay, underlying DGAC, and base respectively on all sections. Moduli of 3,580 MPa, 400 MPa, and 100 MPa were used for the underlying DGAC, base, and subgrade respectively. An intact modulus of 12,000 MPa with a damage of 0.253 was assumed for the underlying DGAC. The same factors for the effects of confining stiffness and nonlinearity of the aggregate base and the subgrade were assumed for all sections.

Damage and cracking were determined at the end of the (simulated) HVS loading, at 458 million ESALs. The values, ranked according to the amount of cracking from best to worst, are shown in Table 4. These rankings are the same for the AR4000 and RAC-G sections, which cracked, and places the third section, which showed some initial cracking (MB-4 45 mm overlay) in one place different from ranking from the HVS tests. These simulation results showed that the differing conditions under the overlays in the HVS sections did not substantially alter their ranking in performance. The simulations also provided an indication of the expected ranking of the sections that showed damage, but were not trafficked to a point where cracking reached the surface.

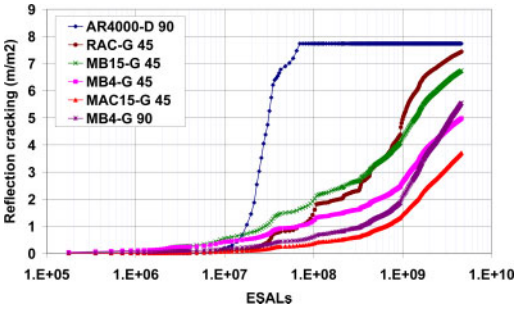

Figure 6. Simulated reflective cracking for identical testing conditions.

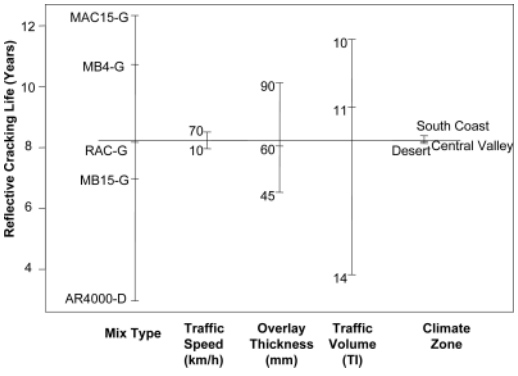

Figure 7. Design plot of reflective cracking life for asphalt overlays on cracked asphalt with using field mixed field compacted fatigue beam results. (Note: TI values are 2.4 million, 5.4 million and 41 million ESALs for TI = 10, 11 and 14, respectively).

The simulated reflective cracking is shown as a function of the number of loads (in ESALs) in Figure 6. The ranking depends to some extent on the number of load applications. The ranking would not change significantly if it was based on the reflective cracking predicted from fatigue damage of the overlay rather than surface cracking.

3.7 *Simulation 6: Extrapolation to field conditions and sensitivity studies*

Simulations were carried out to assess extrapolation of mix performance in the HVS tests to performance in the field. These results provided a preliminary assessment of expected field performance, considering the many limitations of the modeling and need to be checked with results from in-service pavements. An example of average values for reflective cracking life for each variable in the factorial of simulations for overlays on cracked asphalt pavement is shown in Figure 7. It shows that the effect of overlay mix type, climate region, and traffic level are more important than overlay thickness (for the ranges used).

Based on the simulation results, a number of observations were made based on simulations using the field

mixed field compacted materials placed on the HVS test sections:

- The relative ranking with respect to reflective cracking under field conditions was the same as the ranking under HVS test conditions, with the only exception being the RAC-G and MB15-G mixes. The RAC-G performed better than MB15-G in the field simulations but worse in the HVS tests.
- AR4000-D and MB15-G mixes had significantly shorter reflective cracking life under the Desert climate than under South Coast and Central Valley climates. The other mixes did not appear to be sensitive to climate conditions.
- Reflective cracking life was generally not sensitive to an increase in overlay thickness from 45 mm to 90 mm, and increasing the overlay thickness from 45 mm to 90 mm would not necessarily result in a longer reflective cracking life.
- Reflective cracking life decreased as traffic volume increased, but the life decreased at a rate much smaller than the increase in traffic volume.
- Increasing traffic speed from 10 km/h to 70 km/h approximately doubled the reflective cracking life for AR4000-D and MB15-G mixes. However, the reflective cracking life for the MB4-G, MAC15-G, and RAC-G mixes were less sensitive to traffic speed.

4 SUMMARY

This paper has presented a discussion of the synergistic interaction of mechanistic-empirical analysis and accelerated pavement testing. APT is used to calibrate ME analysis models, and calibrated ME analysis can then be used to solve problems with accelerated pavement testing results. These problems particularly occur when APT is used for comparison studies between different pavement alternatives, and include inevitable differences in underlying conditions, construction quality, loading, and environmental control. Calibrated ME analysis can then also be used to extrapolate APT results to a much wider range of conditions in the field than can practically and economically be considered by APT alone. This paper presented a demonstration of this process from an experiment to compare different asphalt overlay treatments for reflective cracking and rutting performance that included six different sets of simulations, from calibration through extrapolation.

ACKNOWLEDGEMENT

This paper describes research activities requested and sponsored by the California Department of Transportation (Caltrans), Division of Research and Innovation. Caltrans sponsorship is gratefully acknowledged. The contents of this paper reflect the views of the authors and do not reflect the official views or policies of the State of California or the Federal Highway Administration.

REFERENCES

ARA Inc., ERES Consultants Division. 2004. *Guide for Mechanistic-Empirical Design of New and Rehabilitated Pavement Structures.* Report to National Cooperative Highway Research Program, Project 1-37A. Washington, DC.

Harvey, J. 2008. Impacts and Benefits of APT: An APT Operator's Perspective. *Proceedings of the 3rd International Conference on Accelerated Pavement Testing*, Madrid, Spain, October.

Jones, D. Harvey, J. and Monismith, C.L. 2007a. *Reflective Cracking Study: Summary Report.* Davis and Berkeley, CA: University of California Pavement Research Center UCPRC-SR-2007-01.

Jones, D., Tsai, B. Ullidtz, P., Wu, R., Harvey, J. and Monismith, C.L. 2007b. *Reflective Cracking Study: Second-Level Analysis Report.* Davis and Berkeley, CA: University of California Pavement Research Center. UCPRC-RR-2007-09.

Jones, D. and Harvey, J. 2007c. *Reflective Cracking Study: HVS Test Section Forensic Report.* Davis and Berkeley, CA: University of California Pavement Research Center. (UCPRC-RR-2007-05).

Jones, D., Harvey, J. and Bressette, T. 2008. An Overview of an Accelerated Pavement Testing Experiment to Assess the Use of Modified binders to Limit Reflective Cracking in Thin Asphalt Concrete Overlays. *Proceedings, 6th RILEM International Conference on Cracking in Pavements*, Chicago, June. pp 45–54.

Thoegersen, F., Busch, C. and Henrichsen, A. 2004. *Mechanistic Design of Semi-Rigid Pavements—An Incremental Approach.* Report 138. Danish Road Institute, Fløng, Denmark.

Ullidtz, P., Harvey, J., Tsai, B. and Monismith, C.L. 2008a. Calibration of Mechanistic–Empirical Models for Flexible Pavements Using the California Heavy Vehicle Simulators. In *Transportation Research Record, 2087.* Washington, DC. Transportation Research Board. pp. 20–28.

Ullidtz, P., Harvey, J. Tsai, B. and Monismith, C.L. 2008b. Calibration of Mechanistic Empirical Models for Flexible Pavements Using the WesTrack Experiment. *Journal of the Association of Asphalt Paving Technologists. Vol. 77*. pp 591–630.

Ullidtz, P., Harvey, J., Basheer, I., Jones, D., Wu, R., Lea, J.D. and Lu, Q. 2010. *CalME*, a Mechanistic-Empirical Program to Analyze and Design Flexible Pavement Rehabilitation. In *Transportation Research Record, No 2153*. Washington, DC. Transportation Research Board. pp 143–152.